Casey Schrader U0951739
Emma Layon U1355443
Gage Allred U1409414
GEOG 4140
April 8th, 2024

Analysis of the Rim Fire in Yosemite and the Future Fire Risk

Introduction

In August of 2013, a 257,314 acre fire ignited in the Stanislaus National Forest in Eastern Central California. This fire, known as the "Rim Fire" spread quickly through the heavily vegetated area, and into portions of the Yosemite National Park. This area of California is frequently exposed to wildfires, putting habitats and communities in danger. This research analyzes the severity and impact of the Rim Fire on the Stanislaus National Forest and Yosemite National Park in an attempt to ascertain the risk of future wildfires in Yosemite. This research provides a noticeable benefit as analyzing past fires and identifying potential hazard zones in the park will allow for better risk assessment and management in order to support emergency preparedness and response, which in turn contributes to the protection of lives and property. This research will especially be beneficial to the National Forest Service and National Park Service, who can then make more well-informed decisions based on the possibilities of future fires on this highly visited area of land.

Research that has been conducted by Westerling et al. (2014) provides insights into the severity and impacts of the Rim Fire on Yosemite National Park. They found that the Rim Fire was one of the largest and most destructive wildfires in California's recorded wildfire history. Additional Research by Miller et al. (2015) emphasizes the importance of assessing future wildfire risks in Yosemite National Park. By analyzing this past fire and identifying potential

hazard zones, this research contributes to more effective risk assessment and management strategies, ultimately aiding in protecting lives and property in these critical landscapes (Westerling et al., 2014; Miller et al., 2015).

Data

This analysis relied heavily on the land cover of the area, as presented in the "Yosemite Park Vegetation" map. This provides crucial data in calculating fire risk, as the flammability of the plant growth in any given area highly impacts its ability to start and spread a fire. Shrublands and grasslands are particularly vulnerable, as well as any coniferous forests, though any area primarily consisting of vegetation will be at least somewhat at risk. Areas directly near roads also have a higher chance of burning due to the potential for fires caused by automobile accidents.

The primary data utilized in our analysis consisted of multispectral images capturing the Yosemite Rim Fire site. These images were acquired by Landsat 8's Operational Land Imager (OLI), featuring nine spectral bands, including near-infrared and shortwave infrared bands needed for the NDMI Equation. The data and images were sourced from the United States Geological Survey's Earth Explorer database. Specifically, we utilized three images from varying dates: August 13, 2013, September 16, 2013, and September 26, 2013.

To create the Yosemite vegetation map, we obtained high-resolution polygons from the vegetation mapping inventory project of Yosemite National Park, accessible within the National Park Service's database. These polygons were derived from color infrared analog photographs collected in 1997 by Photo Science.

For the Yosemite fire risk map, data was acquired from ArcGIS user LeoT_cpe via the ArcGIS online content portal. This user collected population density, per capita income, and median age data from the 2018 U.S. Census, along with Fire Threat Index data from CALFIRE.

Methods

To begin the analysis of the effect of the fire, we acquired multispectral imagery of the area before and after the fire through USGS "Earth Explorer" which provides a database of all NASA Landsat 8 imagery. The dates that were chosen for the before and after photos were August 15th and September 16th. For our first map, we just put the photos side by side so we could see what the land looked like before and after the Rim Fire.

The next map displays the burn severity of the fire. We chose to do a Normalized Vegetation Moisture Index (NDMI) over NDVI for the band arithmetic, as studies have shown that the NDMI is more effective in assessing burn severity than other methods (Veraverbeke et al., 2012, Fornacca et al., 2018). We did band arithmetic on both of the images from August 15th and September 16th and then subtracted the after from the before to get the burn severity.

For the change detection map, we used ArcGIS Pro's change detection tool by plugging photos in. We first created a change detection map for the initial burn to see how the fire immediately affected the land. We used the same photos from August 15th and September 16th, 2013 to do this analysis.

Next, we made another change detection map, using the same change detection tool in ArcGIS Pro. For this analysis, we wanted to see the long term effects of the fire, so we used a photo from after the burn in September 2013, and then a photo from September 2023. This map shows us how the vegetation has grown since the fire.

Then, we made a modified map to emphasize the fire risk in only the surrounding Yosemite area. We used data and features from user LeoT_cpe in ArcGIS online catalog to create a map that emphasizes the fire risk in the Yosemite and surrounding area. This user used a weighted overlay analysis of population density, median age, and per capita income from the

U.S. Census performed in 2018. On top of this, fire threat index data from CALFIRE was laid over. This map will be used to show where fire risk will leave people the most vulnerable.

Results

The true color imagery for August 15, 2013, and September 16, 2013, provides an overview of the extent of the Yosemite Rim Fire. While it provides little new data, it effectively visualizes the consequences of allowing fires like this to occur, perhaps more so than any other representation of specific data could.

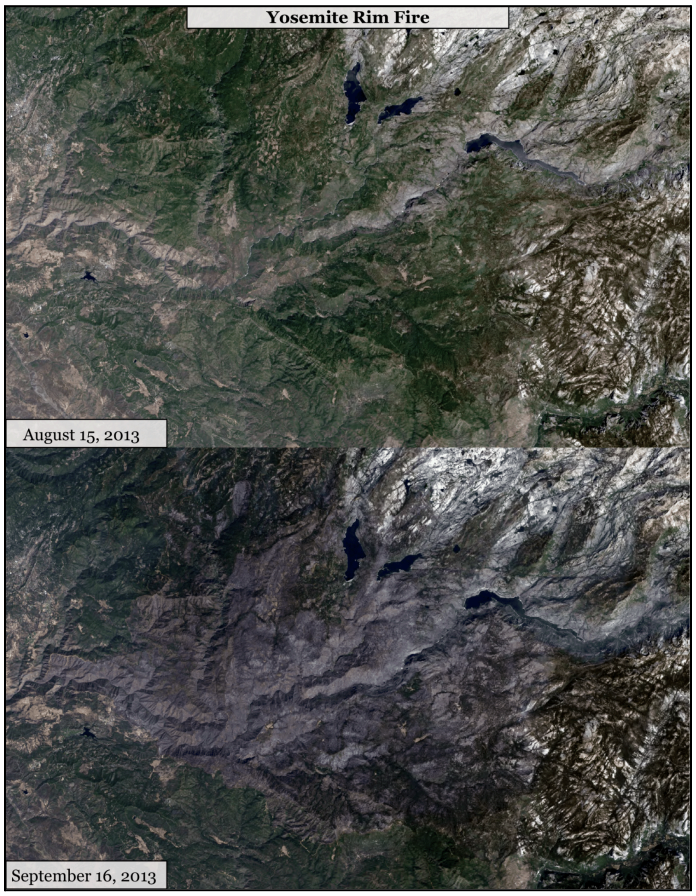

The accompanying burn severity map reveals that while roughly 15 square miles experienced low severity burns, there are significant areas with moderate and high severity burns concentrated within the central zones of the fire.

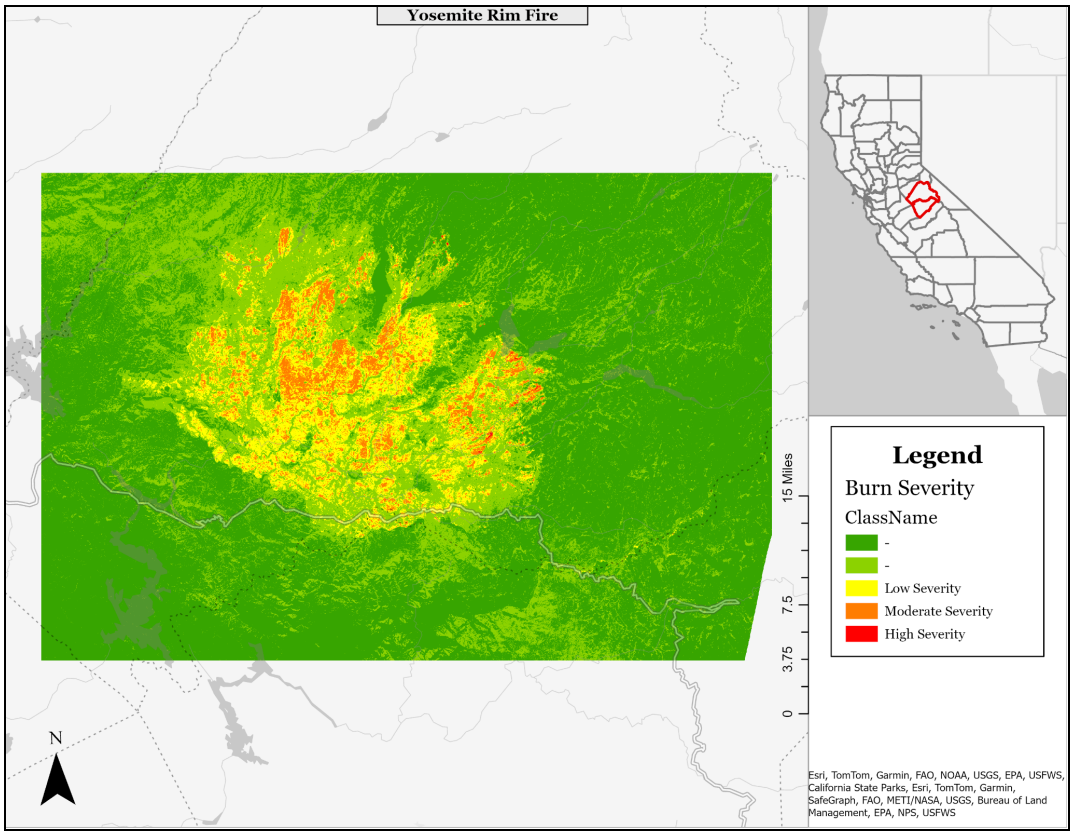

A change detection analysis further highlights regions of heightened severity by displaying the extent of the change in burns between August and September of 2013, with lower values and darker colors representing higher intensities as the value itself represents the health of the area. Another map shows the same change detection in a longer range, between the year of the fire and 2023. This shows much the same results as the first one, even displaying higher change values in some areas. Upon evaluating this map and comparing it to the 2013 burn severity map, it is evident that vegetation in areas with the most severe burns has likely struggled to fully regrow even a decade after the fire. There also may be more measures in place to allow for controlled fires in the area, such that it hasn't been allowed to get overgrown as it may have been before the fire due to the complete prevention of fire beforehand.

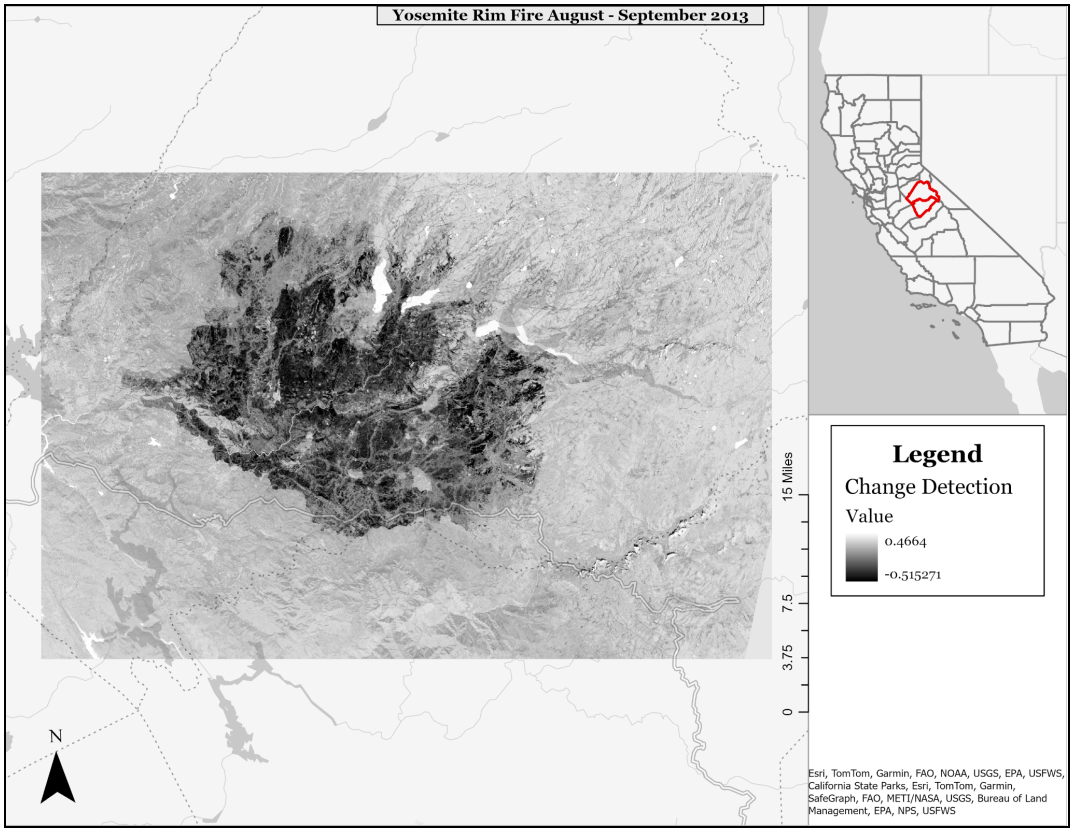
Yosemite Rim Fire August - September 2013
15 Miles
7.5
3.75
0
N
Legend
Change Detection
Value
0.4664
-0.515271
Esri, TomTom, Garmin, FAO, NOAA, USGS, EPA, USFWS, California State Parks, Esri, TomTom, Garmin, SafeGraph, FAO, METI/NASA, USGS, Bureau of Land Management, EPA, NPS, USFWS

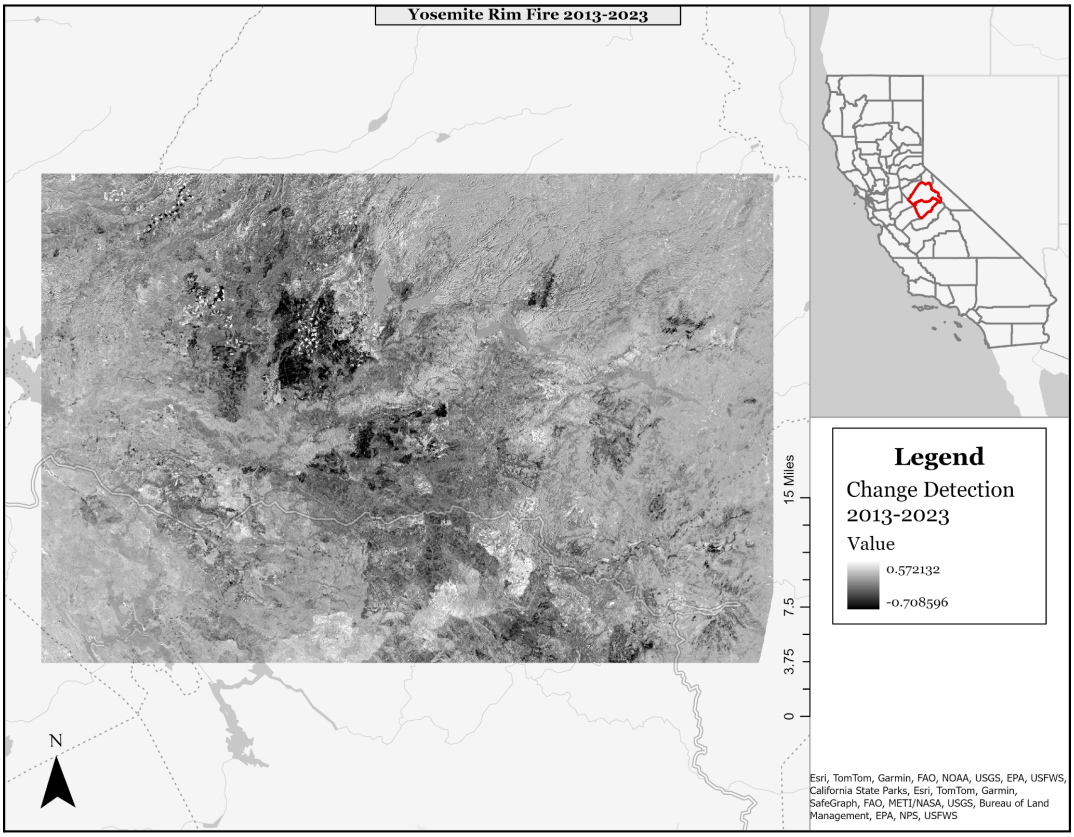
Yosemite Rim Fire 2013-2023
15 Miles
7.5
3.75
0
N
Legend
Change Detection
2013-2023
Value
0.572132
-0.708596
Esri, TomTom, Garmin, FAO, NOAA, USGS, EPA, USFWS, California State Parks, Esri, TomTom, Garmin, SafeGraph, FAO, METI/NASA, USGS, Bureau of Land Management, EPA, NPS, USFWS

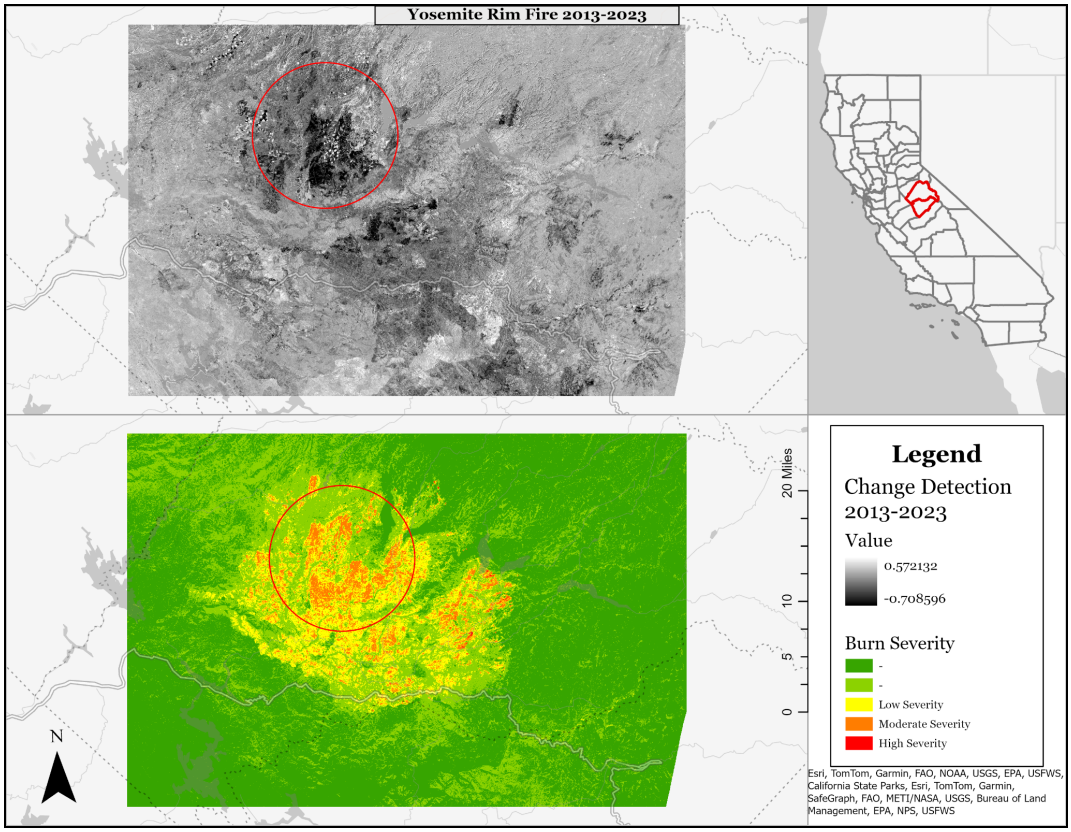

We also generated a map displaying the variation in land cover in the area. While outside the scope of this project, further effort could be invested into the flammability of different vegetation types and incorporated with a map such as this to further pinpoint the likelihood of unwanted fires at any given location in the area.

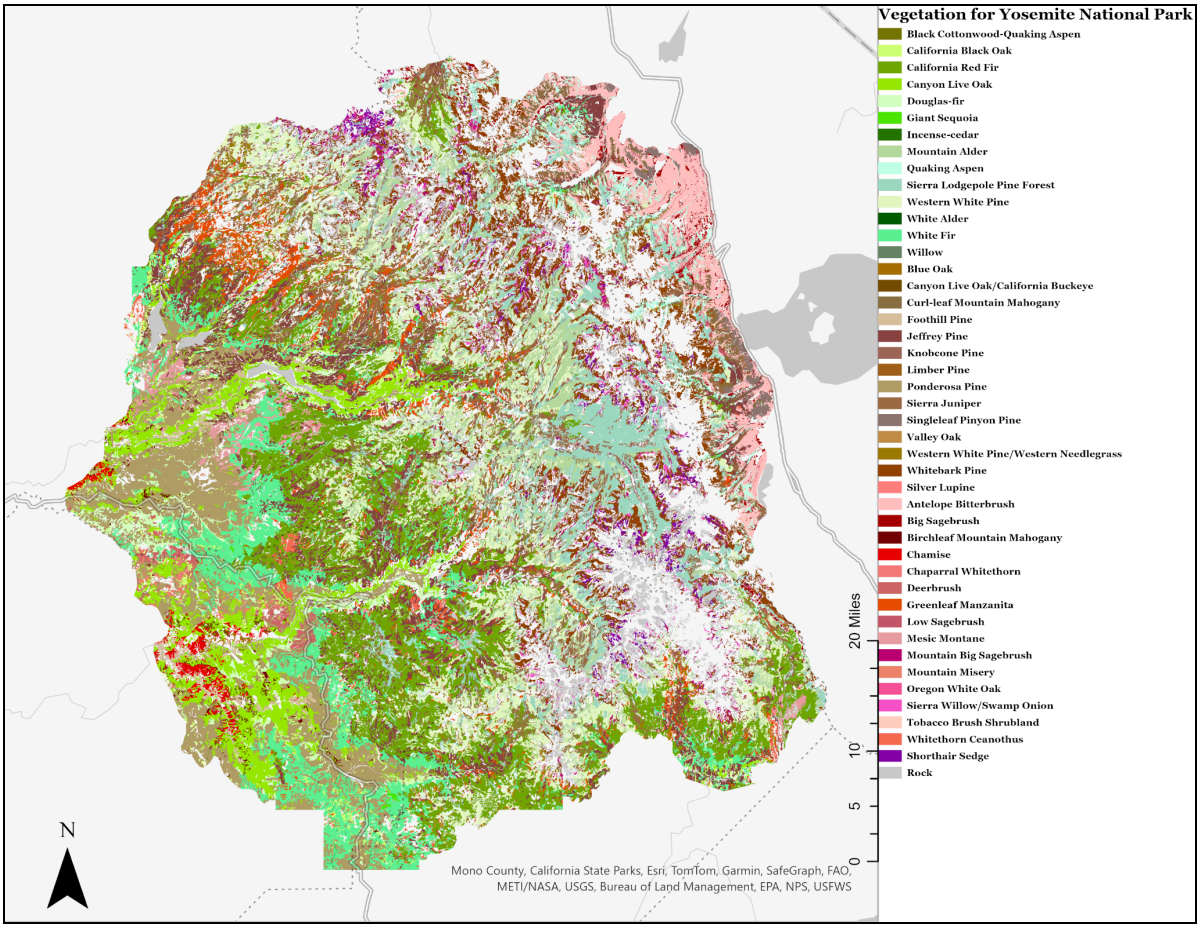
Vegetation for Yosemite National Park
Black Cottonwood-Quaking Aspen
California Black Oak
California Red Fir
Canyon Live Oak
Douglas-fir
Giant Sequoia
Incense-cedar
Mountain Alder
Quaking Aspen
Sierra Lodgepole Pine Forest
Western White Pine
White Alder
White Fir
Willow
Blue Oak
Canyon Live Oak/California Buckeye
Curl-leaf Mountain Mahogany
Foothill Pine
Jeffrey Pine
Knobcone Pine
Limber Pine
Ponderosa Pine
Sierra Juniper
Singleleaf Pinyon Pine
Valley Oak
Western White Pine/Western Needlegrass
Whitebark Pine
Silver Lupine
Antelope Bitterbrush
Big Sagebrush
Birchleaf Mountain Mahogany
Chamise
Chaparral Whitethorn
Deerbrush
Greenleaf Manzanita
Low Sagebrush
Mesic Montane
Mountain Big Sagebrush
Mountain Misery
Oregon White Oak
Sierra Willow/Swamp Onion
Tobacco Brush Shrubland
Whitethorn Ceanothus
Shorthair Sedge
Rock
20 Miles
10
5
0
N
Mono County, California State Parks, Esri, TomTom, Garmin, SafeGraph, FAO, METI/NASA, USGS, Bureau of Land Management, EPA, NPS, USFWS

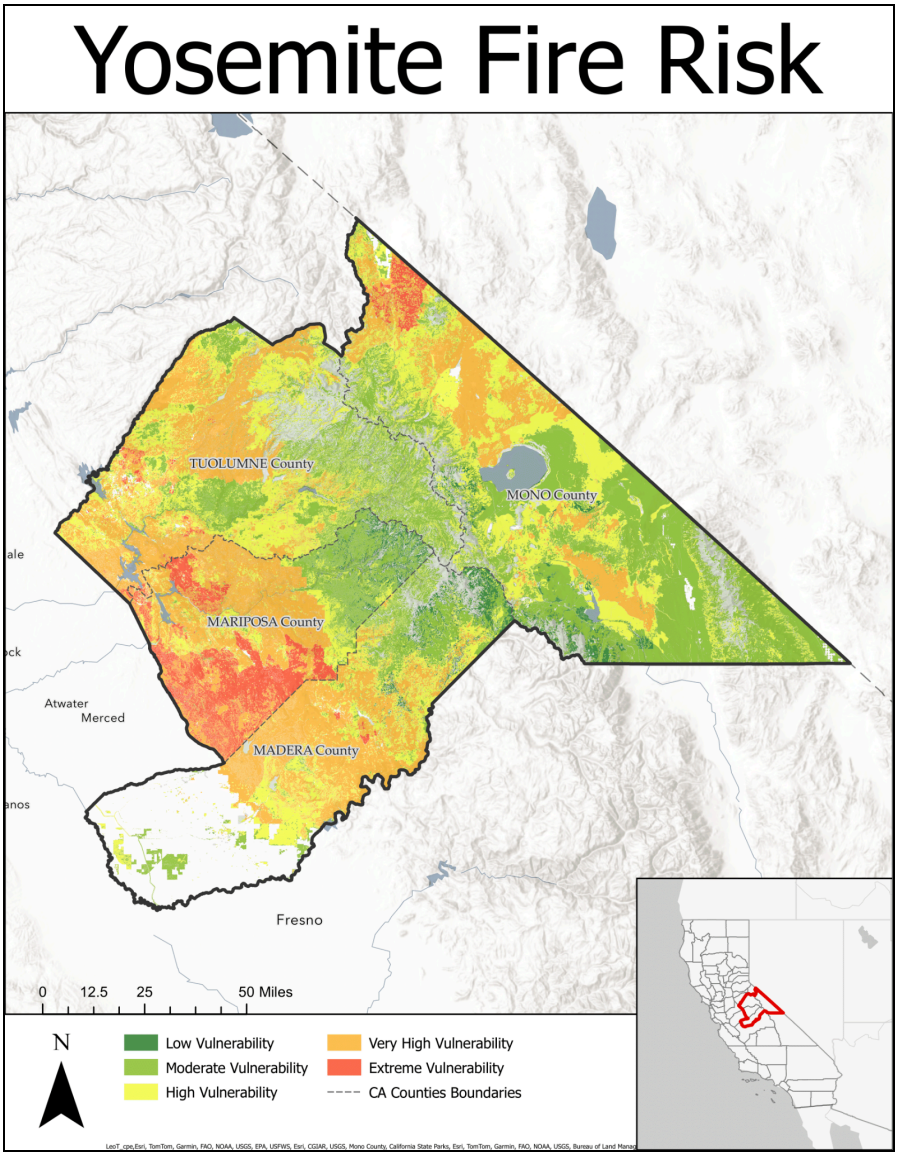

Finally, we have a map displaying fire vulnerability for the wider area including Yosemite Park. This combines several demographics-related factors to display the areas in which fires could have an excessive impact, though not necessarily where fires are most likely to occur.

Conclusion

The analysis of the 2013 Yosemite Rim Fire provides an insight on the lasting impacts of wildfires and the timeline for natural recovery. Revisiting the fire-affected area in the future would offer further insights into the correlation between burn severity and vegetation regrowth.

Additionally, applying NDVI arithmetic instead of NDMI for change detection could enhance the analysis by focusing on vegetation amount and health rather than moisture and burn fuel potential.

Considering our examination of this fire alongside fire risk data from neighboring counties, it's evident that a similar event could not only harm vegetation but also endanger residents. Therefore, it's crucial to evaluate these risks fully and implement preventive measures to avoid future fires and protect both ecosystems and communities.

Citations

Fornacca, Davide, Guopeng Ren, and Wen Xiao. 2018. "Evaluating the Best Spectral Indices for the Detection of Burn Scars at Several Post-Fire Dates in a Mountainous Region of Northwest Yunnan, China" Remote Sensing 10, no. 8: 1196. https://doi.org/10.3390/rs10081196

Miller, J. D., Safford, H. D., Crimmins, M., & Thode, A. E. (2015). Quantitative evidence for increasing forest fire severity in the Sierra Nevada and southern Cascade Mountains, California and Nevada, USA. Ecosystems, 12(1), 16-32.

Veraverbeke, S., Lhermitte, S., Verstraeten, W.W., Goossens, R. (2012), Evaluation of pre/post-fire differenced spectral indices for assessing burn severity in a Mediterranean environment with Landsat Thematic Mapper. International Journal of Remote Sensing, vol. 32(12), 3521-3537.

Westerling, A. L., Hidalgo, H. G., Cayan, D. R., & Swetnam, T. W. (2014). Warming and earlier spring increase western US forest wildfire activity. Science, 313(5789), 940-943.